Catalysis Today 158 (2010) 186–196

Contents lists available at ScienceDirect

Catalysis Today

journal homepage: www.elsevier.com/locate/cattod

Monte Carlo modeling of the enantioselective adsorption of propylene oxide on 1-(1-naphthyl)ethylamine-modified Pt(1 1 1) surfaces

J.L. Sales [a], V. Gargiulo [a], I. Lee [b], F. Zaera [b], G. Zgrablich [a,*]

[a] Instituto de Física Aplicada (INFAP), CONICET-UNSL, San Luis, Argentina
[b] University of Califórnia, Riverside, USA

ARTICLE INFO

Article history:
Available online 10 May 2010

Keywords:
Enantioselective adsorption
Propylene oxide
1-(1-Naphthyl)ethylamine
Monte Carlo simulation

ABSTRACT

Molecular models are proposed to study the enantioselective adsorption of enantiopure propylene oxide (PO) species on platinum surfaces modified by preadsorption of enantiopure 1-(1-naphthyl)ethylamine (NEA) chiral species. This system has been studied experimentally recently [12], and has been found to present a very complex behavior. In this report we show that the observed behavior cannot be explained simply through pair-wise interactions between adsorbed molecules, but rather requires the consideration of cooperative effects arising in some particular local configurations. Starting from a very simple model, kinetic Monte Carlo simulations were used in order to predict the thermal programmed desorption spectra of PO from template surfaces with different NEA coverages. As these predictions were analyzed, more complex conditions were seen to be necessary for a satisfactory reproduction of experimental data. The final model developed in this work does account for many of the trends observed experimentally in the PO + NEA/Pt(1 1 1) system, but is intended to be only a first step toward the understanding of the complex behavior reported at a molecular level. Throughout the development of our model, it was possible to identify some basic necessary conditions in connection with cooperative effects required to reproduce the experimental data.

1. Introduction

Chiral molecules are found in two enantiomeric forms, two mirror-image not superimposable structures. The two enantiomers, (R) and (S), of a chiral molecule often have identical chemical and physical properties, but they do display different chemistry when interacting with other chiral elements despite having the same chemical composition. This is of fundamental importance in drug design, since it has been found that, while one enantiomer of a drug may be completely effective for the treatment of a given disease, the other can be very harmful. During the last decade considerable effort has been directed toward developing new methods to obtain enantiomerically pure compounds. Special interest has been manifested in finding heterogeneous chiral catalysis methodology to replace existing homogeneous chiral catalysis processes. Thus, understanding enantioselective adsorption, the first step in heterogeneous chiral catalysis, may be of great relevance to the design of new drug synthesis, in particular if it can lead to selectively produce one of the two enantiomers of a chiral molecule.

There are currently thought to be two main mechanisms by which a chiral adsorbate may modify and impart enantioselectivity to a heterogeneous catalyst:

(a) One-to-one mechanism
One chiral modifier is anchored to a surface in such a way it modifies an adjacent site and imparts enantioselectivity to the adsorption of a reactant molecule via a direct one-to-one modifier–reactant interaction. This kind of mechanism may operate in the case of large chiral modifiers such as cinchonidine [1,2]. The effectiveness in chiral modification in this case is mostly dependent on the molecular characteristics of the individual modifier molecules [3,4].
(b) Template mechanism
In this case the substrate is partially covered by a modifier of a given chirality, say *R*, forming a structure that act as a "template" [5,6]. This template may present an extended chiral structure that may selectively affect the subsequent adsorption of other prochiral molecules. This kind of mechanism appears to apply to the systems studied in Refs. [7–11].

Given that the precise structural relationship between a templating overlayer and the probe molecules is not yet well understood, advances in the study of the problem can be made by taking

* Corresponding author.
E-mail address: giorgio.unsl@gmail.com (G. Zgrablich).

0920-5861/$ – see front matter © 2010 Elsevier B.V. All rights reserved.
doi:10.1016/j.cattod.2010.04.021

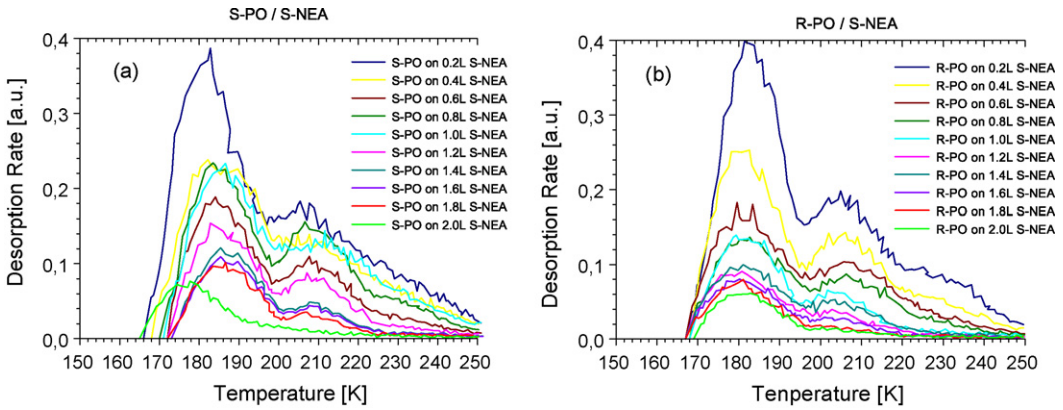

Fig. 1. Experimental TPD spectra for the desorption of (S)-PO (a), and (R)-PO (b), from a Pt(1 1 1) surface previously dosed with different amounts of (S)-NEA ranging from 0.2 to 2.0 L [12].

advantage of the fact that the two mechanisms described above should yield different dependencies of enantioselectivity as a function of coverage of the chiral one-to-one modifier or templating species. In particular, enantioselectivity based on the modification of the substrate by chemisorption of a templating chiral species is expected to yield a significant enantioselective excess only in a narrow range of coverage of the templating species [7–11]. There have been recent interesting lattice-gas studies in the literature [13–15] where it has been shown how enantioselectivity of a chiral species could arise on a substrate with a pattern of strong and weak adsorbing sites. This mechanism may certainly apply in many cases. However, there are other systems, especially those studied experimentally in Refs. [7,10,11], where the cause of enantioselectivity in adsorption cannot be due to a difference in adsorption energy of different sites. In those experiments, one enantiomer of a chiral probe molecule is adsorbed on a surface previously templated via preadsorption of a specific enantiomer, (R) or (S), of another chiral species until reaching saturation. The enantioselectivity of the templated surface in those systems is manifested by differences in yields of adsortion energetics between the two enantiomers, (R) vs. (S), of the probe molecule: (R)/(R) and (S)/(S) pairings display different behavior in temperature programmed desorption (TPD) experiments compared to that seen with R-S and S-R pairings. The ratio between the desorption yields, for instance Yield[(R)/(R)]/Yield[(R)/(S)], reflects the enantioselectivity of the template surface. In these circumstances, a difference in adorption energy between the (R)/(R) and (R)/(S) pairings would perhaps affect the adsorption kinetics. However, since both enantiomers are adsorbed until saturation is reached, no measurable differences in yield would be expected. Therefore, the behavior of systems like those studied in Refs. [7,10,11] needs to be explained on the basis of a different mechanism.

In the present study we focus on the enantioselective adsorption of propylene oxide (PO) on Pt surfaces modified by the preadsorption of 1-(1-naphthyl)ethylamine (NEA) [12] and propose a number of increasingly more complex models that may serve as a starting point toward a better understanding of the experimental observations at a molecular level.

Some of the key experimental data from thermal programmed desorption (TPD) spectra obtained using both (R)- and (S)-PO, as a probe molecule on Pt(1 1 1) surfaces previously templated with different coverages of (S)-NEA, expressed in Langmuir units, are shown in Figs. 1 and 2 [12]. These include integrated coverages and enantioselectivity data. The behavior seen in these TPD spectra is quite complex: the desorption traces display two well-separated groups of peaks at temperatures around approximately 180 and 210 K, respectively, indicating the presence of two energetically distinct desorption states. One of the most surprising features of these TPD spectra is that, as the NEA coverage on the surface increases steadily, the PO coverage for one of the enantiomers does

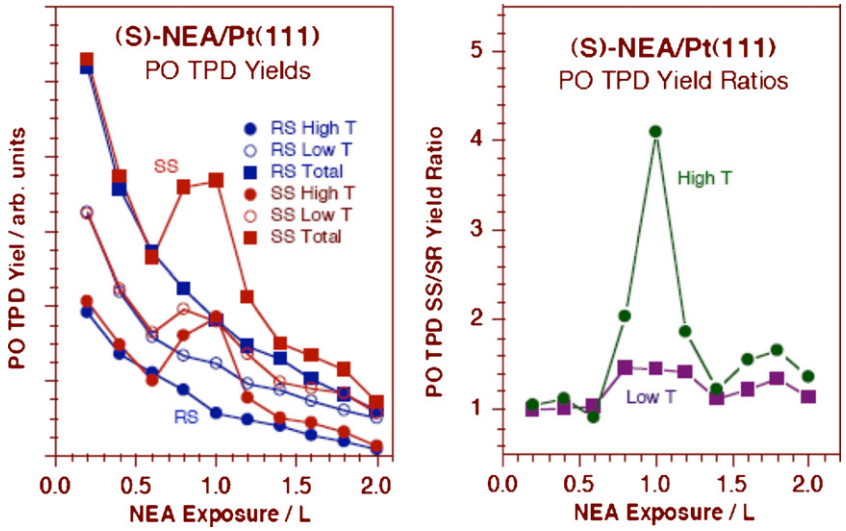

Fig. 2. (a): Integrated PO yields obtained from the experimental TPD spectra in Fig. 1 (left), and (b): corresponding [(S)-PO/(S)-NEA]/[(R)-PO/(S)-NEA] enantioselectivity ratios (right).

not follow a uniform decreasing pattern. Indeed, the PO TPD yield for the (S)-PO/(S)-NEA pairing does decrease with NEA coverage at low NEA coverage, but then suddenly increases at intermediate coverages before it decreases again after (S)-NEA exposures above approximately 1.0 L. We will label this behavior as a "regression effect", and note again that it occurs only for (S)-PO, i.e., with the PO of the same chirality of the NEA modifier. This regression effect can already be seen clearly in the raw data in Figs. 1 and 2 (a), and it is responsible for the enantioselectivity peaks shown in Fig. 2(b). Nevertheless, enantioselectivity peaks may also be seen in cases where this regression effect is not operative, as we shall see below. In our analysis of these experimental data we shall not take into account the high NEA coverage, small, enantioselectivity peaks, since in that coverage region the number of PO molecules on the surface is small, and that introduces a high level of noise in the experimental measurements.

Several attempts were made here to simulate the experimental results on the base of pair-wise interactions between PO and NEA molecules on the surface, but they all failed completely in reproducing even in the crudest way some of the characteristics of the spectra. We therefore concluded that the observed behavior must be the result of a cooperative effect. We hypothesize that, under the presence of some configurations of (S)-NEA and PO, the surface energetics is locally modified in such a way as to become selective toward the (S)-PO enantiomer. Moreover, it was also established that the proposal of certain forbidden sites on the surface for the adsorption of PO is necessary to reproduce the observed regression effect in the TPD spectra.

With these considerations in mind, we now propose and discuss some cooperative models, progressing from the simplest one and adding more complex conditions as they are proven necessary in order to reproduce experimental data, in order to establish a basis of necessary conditions for the understanding of the behavior of this complex system. In these models surface diffusion of PO was not taken into account since several tests indicated that this process did not affect the results appreciably.

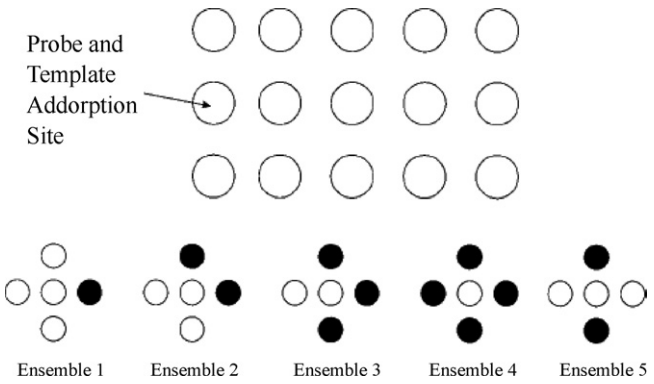

Fig. 3. Representation of all possible ensembles, or configurations of occupied NEA sites around a central empty site available for PO adsorption, used in Model 1, according to the ideas advanced in Refs. [8,9]. The full circles represent adsorbed NEA molecules, the hollow circles empty sites.

2. Model 1

Our simplest cooperative model is based on the ideas already advanced in Refs. [8,9]. According to these ideas, the sites for adsorption of the probe molecules B (in our case PO) may be imbedded in one of 5 possible configurations (ensembles) of nearest-neighbor adsorbed modifier (or template) molecules A (in our case NEA), as shown in Fig. 3. One or more of these configurations may locally modify the energetics of the surface in such a way as to render the adsorbing site selective for the adsorption of one

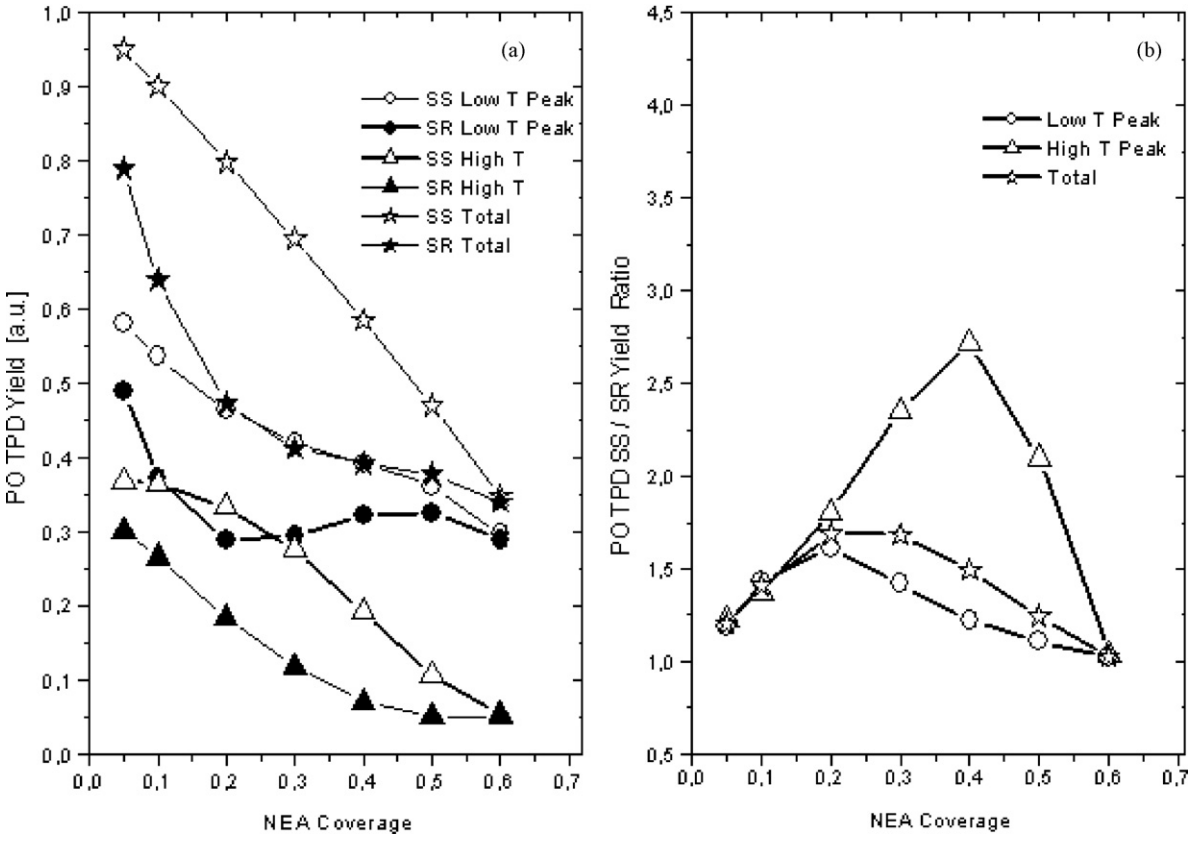

Fig. 4. Integrated PO yields (a) and enantioselectivity ratios (b) calculated using Model 1 with the following assumptions: Ensemble 1 selective and strong for (S)-PO adsorption, Ensemble 4 selective and strong for (R)-PO adsorption.

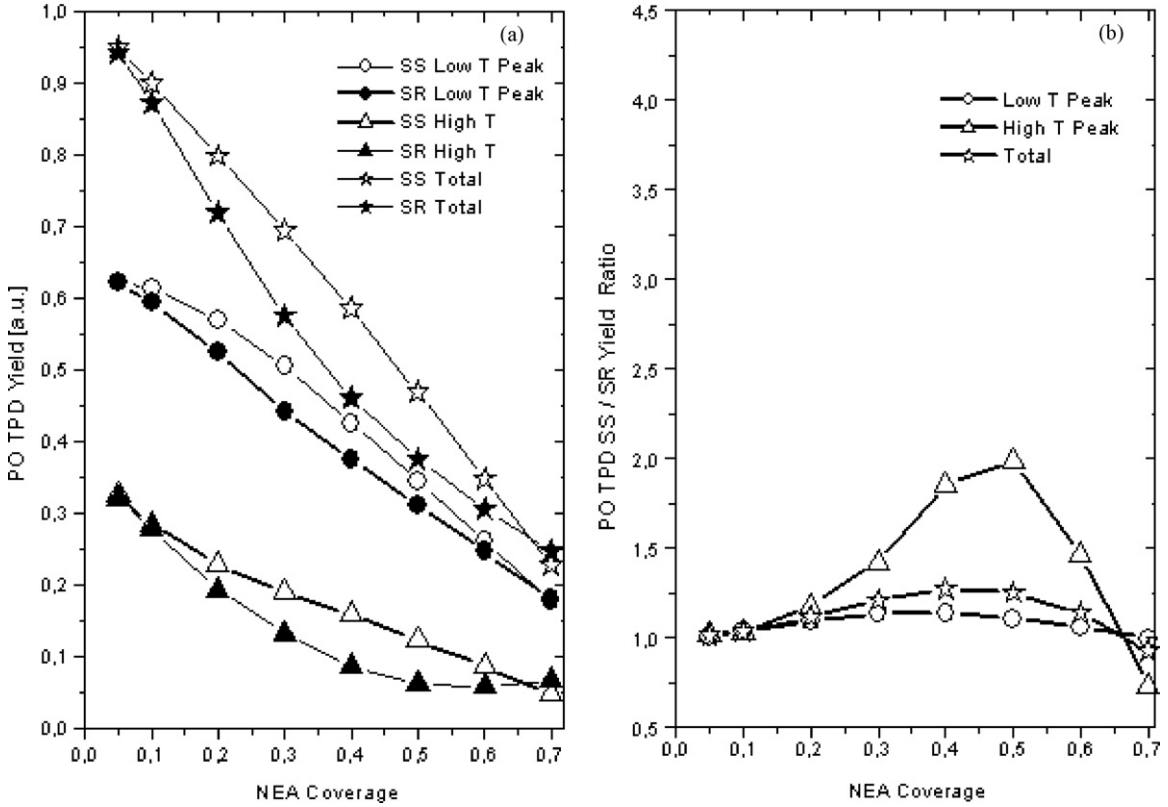

Fig. 5. Integrated PO yields (a) and enantioselectivity ratios (b) calculated using Model 1 with the following assumptions: Ensemble 2 selective and strong for (S)-PO adsorption, Ensemble 4 selective and strong for (R)-PO adsorption.

of the enantiomers, (R) or (S), of the probe molecule, not allowing the adsorption of the other enantiomer. Each of these ensembles produces a different behavior of the system in terms of enantioselectivity. It was found that only Ensembles 1 and 2 are able to give a relatively high enantioselectivity at intermediate coverage. Accordingly, each of these two ensembles was subsequently tested in terms of their contribution to the enantioselective behavior of our system.

Based on initial observations of the simulated TPD spectra obtained for the PO + (S)-NEA/Pt(1 1 1) system, the need to make two assumptions in the initial model was determined:

(a) Both "strong" and "weak" adsorbing sites on the surface are needed in order to account for the two well-separated TPD peaks seen with both (S)-PO and (R)-PO. The strong sites may be generated by the extra binding energy associated with PO adsorbed on a selective site. In our study we found that the adsorption energy for PO on a strong (selective) site is −13.75 kcal/mol, while that for a weak (any other) site is −11.9 kcal/mol, independently of the number of neighboring adsorbed NEA.
(b) A mechanism is required to account for the retention of (R)-PO on the surface at high temperatures, otherwise the (S)-PO/(R)-PO enantioselectivity ratio would increase indefinitely as the NEA coverage increases. This can be properly taken into account by considering Ensemble 4 in Fig. 3 as selective (and therefore strong) for (R)-PO adsorption.

The first, and simplest, model used in our simulations was therefore established as follows: the surface was represented by an effective square lattice where (S)-NEA was adsorbed at random up to a given coverage. Ensemble 1 was considered selective and strong for the adsorption of (S)-PO while Ensemble 4 was selective and strong for the adsorption of (R)-PO. For each modified surface (with a given (S)-NEA coverage), random adsorption processes for (S)-PO and (R)-PO were simulated using a Monte Carlo method up to saturation, and afterwards TPD spectra were simulated following a procedure outlined in Ref. [16]. Finally, integrated coverage and enantioselectivity were obtained from the TPD spectra. Fig. 4(a) and (b) show the integrated yields and enantioselectivity curves, respectively, obtained from this analysis as a function of (S)-NEA coverage. Notice that the main characteristics of the TPD traces, in particular the regression effect, could not be reproduced with this model. More specifically, the low- and high-temperature enantioselectivity peaks occur at significantly different NEA coverages (0.2 and 0.4, respectively), not a trend observed experimentally. This is an effect of the way the strong sites were defined in assumption

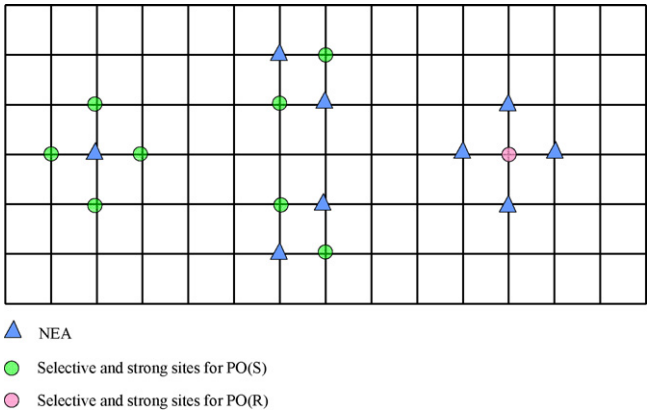

Fig. 6. Representation of selective and strong ensembles for Model 1 combining the two previous assumptions: Ensembles 1 and 2 selective and strong for (S)-PO adsorption, Ensemble 4 selective and strong for (R)-PO adsorption.

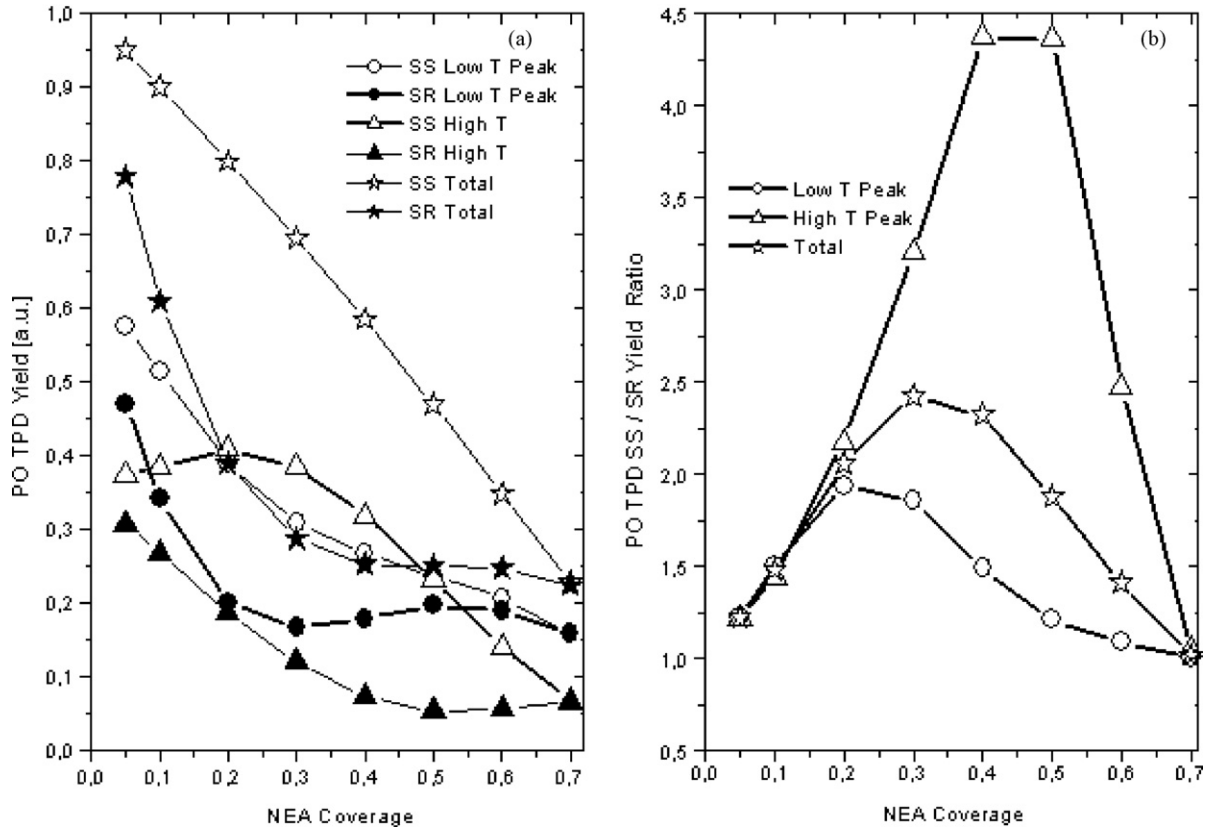

Fig. 7. Integrated PO yields (a) and enantioselectivity ratios (b) calculated using Model 1 with the following assumptions: Ensembles 1 and 2 selective and strong for (S)-PO adsorption, Ensemble 4 selective and strong for (R)-PO adsorption.

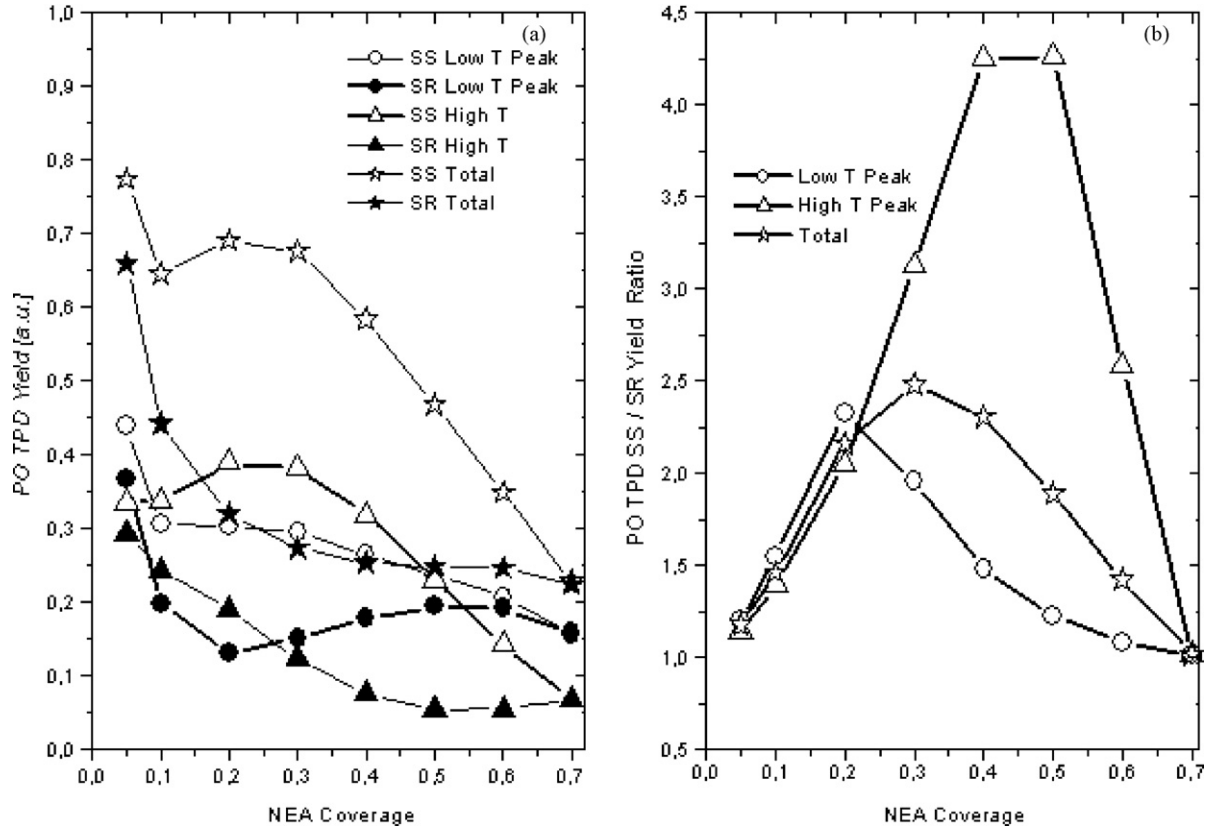

Fig. 8. Integrated PO yields (a) and enantioselectivity ratios (b) calculated using the final version of Model 1 with the inclusion of forbidden sites for the adsorption of PO.

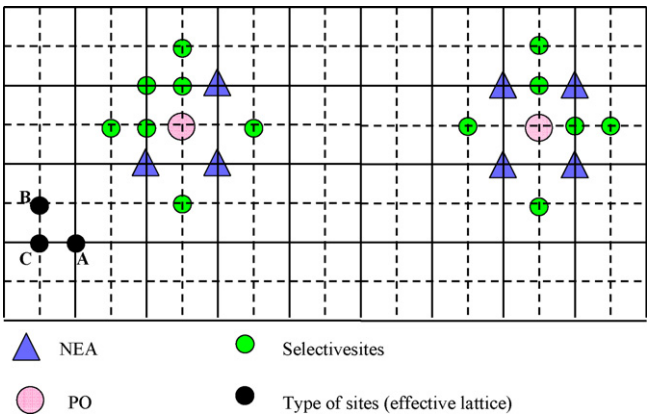

Fig. 9. Representation of the effective lattice used in Model 2 showing some examples of configurations with selective sites deriving from the application of Rule 1.

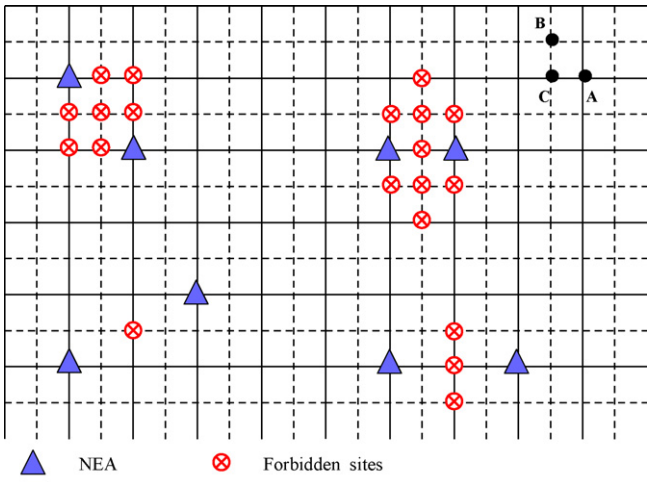

Fig. 11. Some configurations of adsorbed molecules giving rise to forbidden sites for PO adsorption at low coverage, illustrating Rule 2.

(a) above. A change in the model is therefore required in which the strong sites are separated from the selective sites. This is what was done in our Model 2, as discussed later on.

At this stage, a modification to Model 1 was made where Ensemble 2 was made the selective one for (S)-PO adsorption; all other assumptions were kept unchanged. The results from our modeling using this alternative are summarized in Fig. 5. The behavior observed here is similar to that reported in Fig. 4, except for shifts in the enantioselectivity peaks positions and decreases in their values to higher NEA coverages.

In order to increase the value of the selectivity estimated by our modeling, a second modification to Model 1 was advanced where Ensembles 1 and 2 were made both selective for (S)-PO, in effect a combination of the two previous alternatives. Again, all other assumptions were kept unchanged. The different sites available for adsorption in this model are represented in Fig. 6, and the behavior predicted in Fig. 7. Again, it can be seen that the behavior of the TPD spectra is not satisfactory, although a small regression effect did developed in the high-temperature peak. Still the low- and high-temperature enantioselectivity peaks do not appear at the same NEA coverage, even if their intensities now approaches the observed magnitudes.

A slight improvement to this last alternative was introduced next were forbidden sites for PO adsorption were incorporated in order to enhance the regression effect. Those forbidden sites were defined by the following rule: a site surrounded by 2 or more NEA adsorbates in positions of up to 4th-order neighbors away which is not a selective site is forbidden for the adsorption of both PO enan-

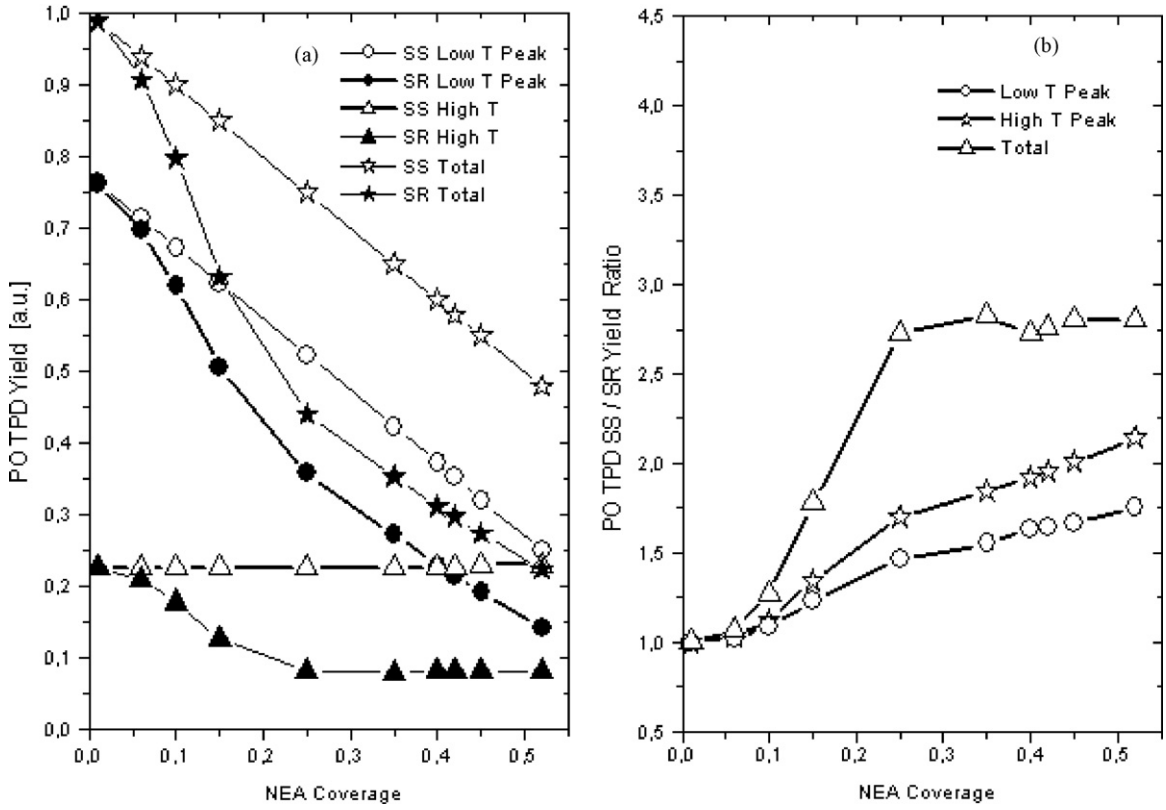

Fig. 10. Integrated PO yields (a) and enantioselectivity ratios (b) calculated using Model 2 with Rule 1.

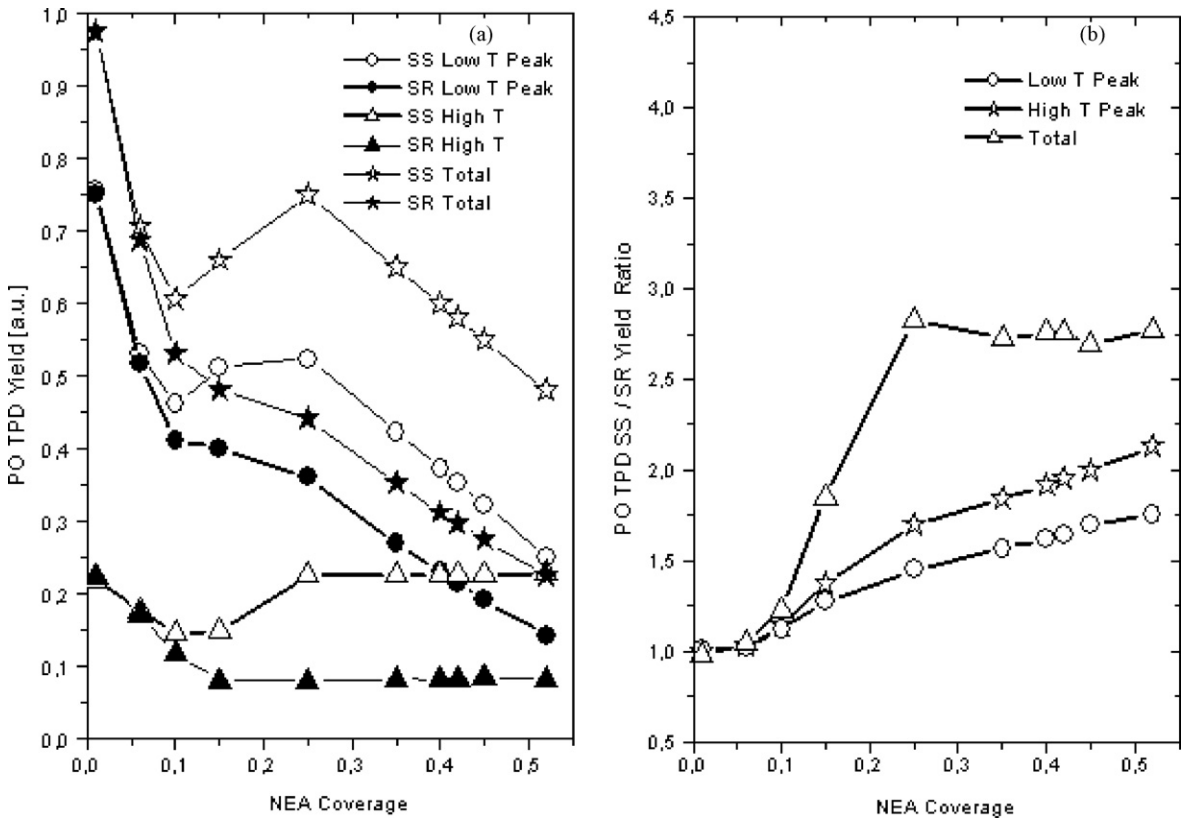

Fig. 12. Integrated PO yields (a) and enantioselectivity ratios (b) calculated using Model 2 with Rules 1 and 2.

tiomers, (R) and (S). This last addition defines what we here will call Model 1. Its predictions are shown in Fig. 8. As we can appreciate, Model 1 can be used as a simple, but still crude, qualitative model to describe the main features of the experimental data from this system. However, contrasting Fig. 8(a) with Fig. 2 indicates that the predicted TPD spectra are still far from being satisfactory. The estimated enantioselectivity intensity values are satisfactory, but their positioning with respect to the NEA coverage still shows significant deviations.

3. Model 2

In analyzing Fig. 8(a), it can seen that the cause for the shift of the low-temperature selectivity peak in the simulations toward low NEA coverages is the fast desorption of (R)-PO at low temperatures and low NEA coverages. A different effective lattice is therefore needed where strong sites for PO adsorption are present independently of those associated with selective adsorption. Moreover, in order to reproduce satisfactorily the regression effect, a more complex effective lattice is required where selective and forbidden sites can be created upon the development of some special configurations arising as PO adsorbs, a consequence of a synergetic process between the adsorbed PO and NEA as suggested in Ref. [12].

Based on these considerations a new proposal was advanced where the surface was considered as an effective lattice composed by two square sub-lattices, indicated by full and broken lines in Fig. 9, respectively. In this scheme there are three types of sites:

Sites A, in the intersections of two full lines, which are assumed to be weak sites for PO adsorption.
Sites B, in the intersections of two broken lines, made strong sites for PO.
Sites C, in the intersections of a broken line with a full line, made weak sites for PO.

The adsorption energies (W) for PO on these sites (A–C) were set as W(B) = −13.75 kcal/mol and W(A,C) = −11.9 kcal/mol. These adsorption energies were determined such that the desorption peaks in TPD spectra would occur at the right temperatures. Both PO and NEA molecules each occupy a single site on the effective lattice. At low coverage, NEA is adsorbed randomly on A sites, until reaching a coverage of 25% of saturation, at which point these sites are all full and the NEA can then be adsorbed randomly on C sites, perhaps in a different (tilted) configuration that occupies less surface area, as also suggested in [12].

The choice of A, B and C sites was not made arbitrarily, but in fact emerged from the following additional considerations:

(a) Because the densities of A, B, and C sites are 0.25, 0.25 and 0.5, respectively, if NEA were allowed to adsorb on B (strong) sites,

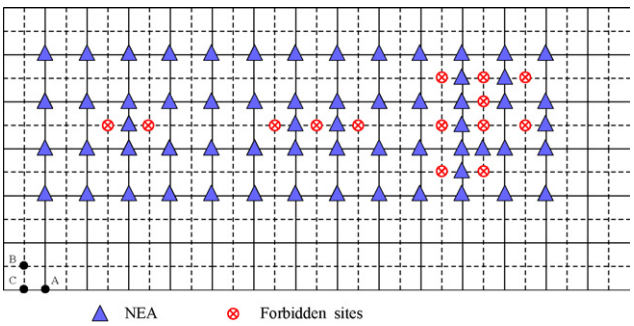

Fig. 13. Some configurations of adsorbed molecules giving rise to forbidden sites for PO adsorption at high coverage, illustrating Rule 3.

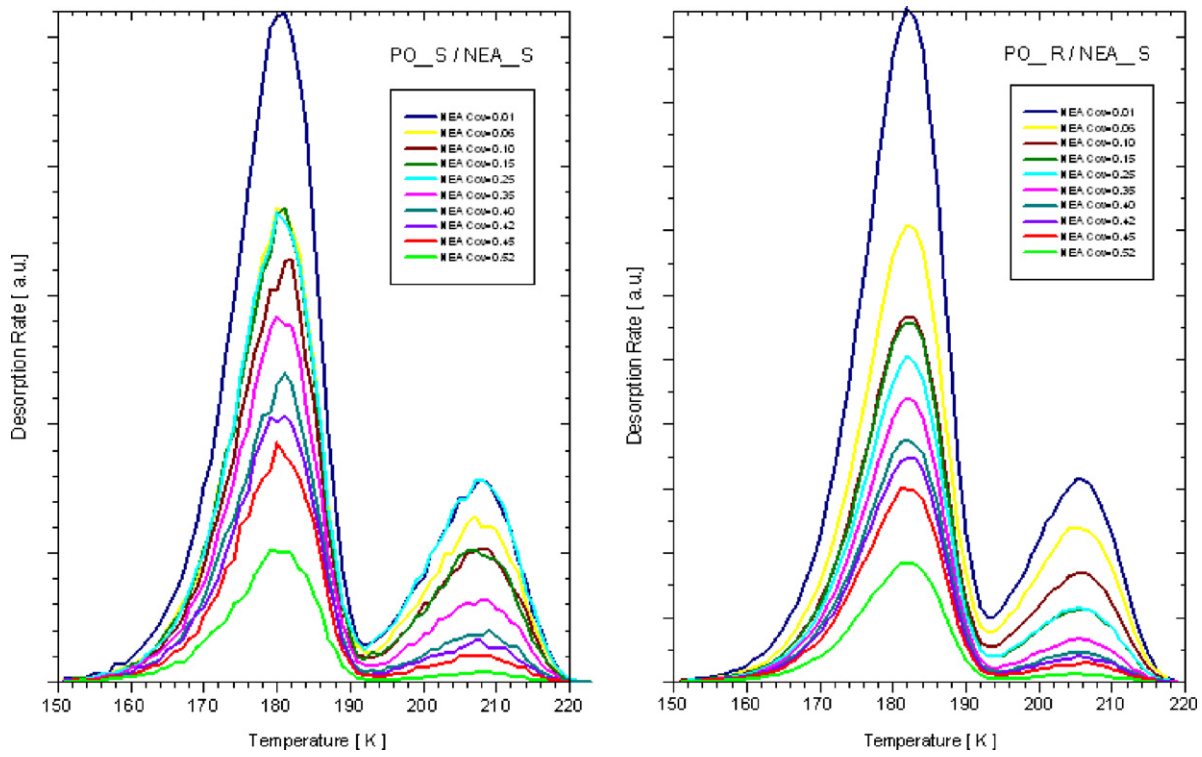

Fig. 14. PO TPD spectra for Model 2 with Rules 1, 2 and 3.

for NEA coverage >0.25 the number of C (weak) sites available for the adsorption of PO would not change with NEA coverage. Therefore, no variation in PO coverage could be induced in the low-temperature peak of the TPD spectra.

(b) If B sites were weak and C sites strong, given that the density of C sites is double that of B sites, the intensity of desorption peaks at high temperature in TPD spectra would be much larger. In contrast, the experimental spectra in Fig. 1 show that the low-temperature peak is always bigger than the high-temperature peak, at all NEA coverages.

We now define the synergetic mechanism through which enantioselective sites are generated. The type of configuration needed and the number of enantioselective sites generated must be such

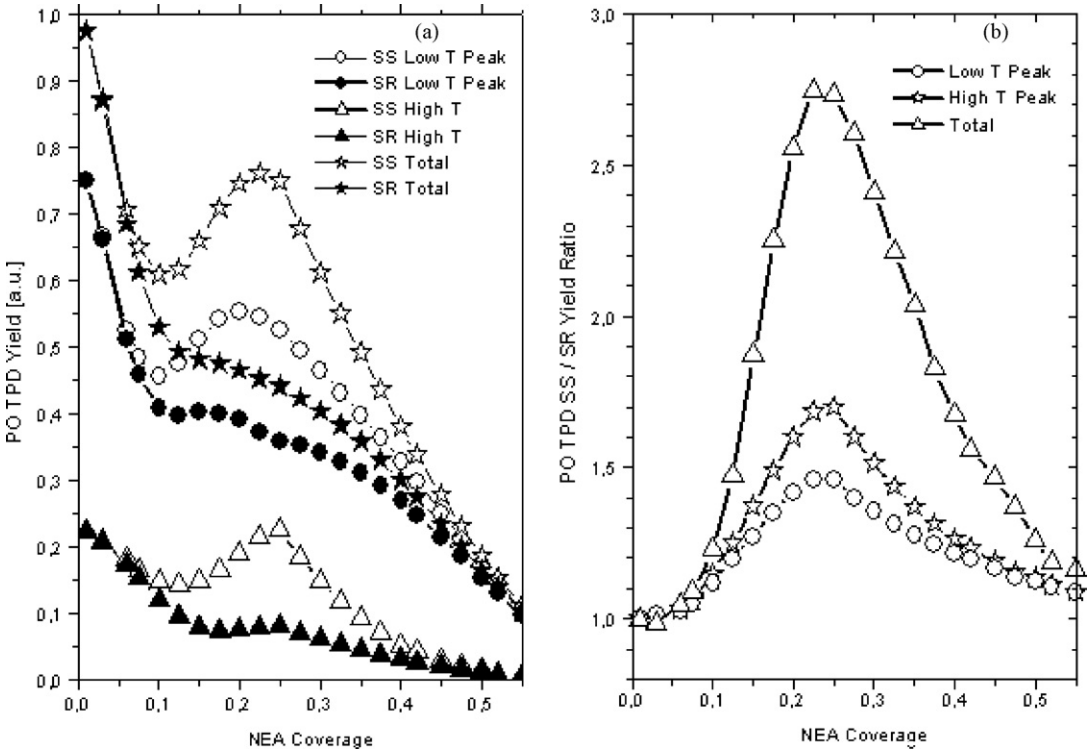

Fig. 15. Integrated PO yields (a) and enantioselectivity ratios (b) calculated using Model 2 with Rules 1, 2 and 3.

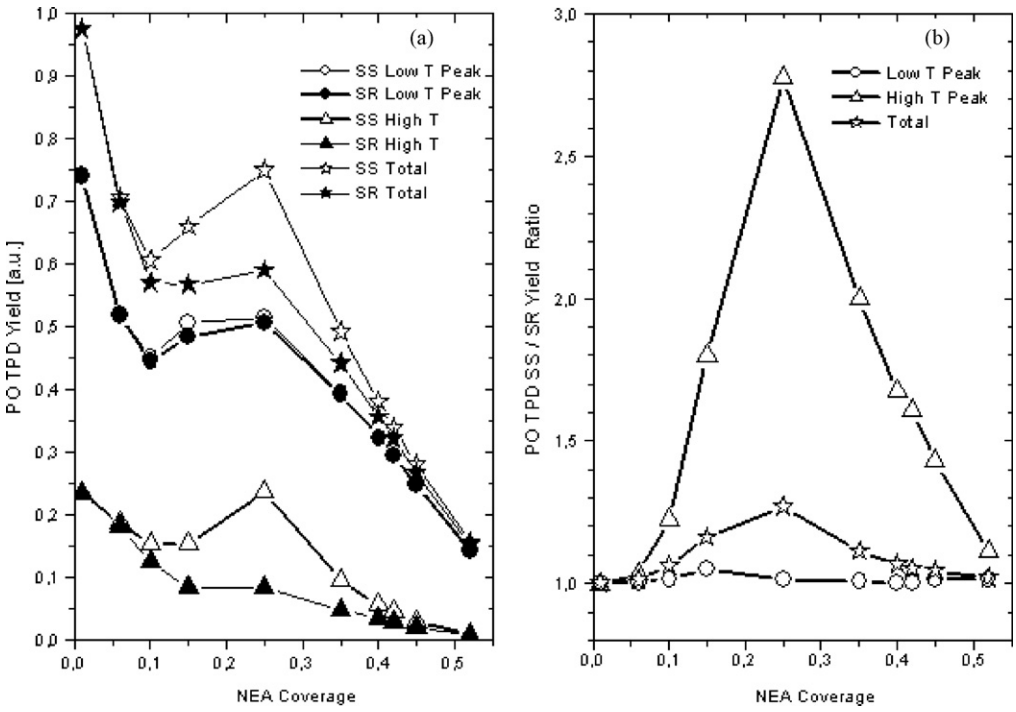

Fig. 16. Effect of relaxing Rule 1 to Rule 1a on the integrated spectra (a) and selectivity curves (b).

that an appropriate growth of the enantioselectivity peaks are obtained. Many simulations were carried out to test different configurations until the following rule was identified for enantioselective sites:

Rule 1

If a PO is adsorbed at a site surrounded by 3 or more 2nd neighbor NEAs, then 2 1st neighbor sites (chosen at random) and all 2nd and 3rd neighbor empty sites become enatioselective for (S)-PO. In addition, the PO adsorbed on that site becomes strongly bounded to the surface.

Examples of some (but not all) enantioselective configurations following this rule can be visualized in Fig. 9. Later on we shall discuss the effects of some modifications to this rule.

Initial simulations with this model were carried out where no forbidden sites were included. Fig. 10 shows the predicted trends in yields and enantioselectivities. It can be appreciated that the initial behavior obtained in terms of PO yields and enantioselectivity is satisfactory. However, no regression effect was reproduced, and the enantioselectivity does not decrease at high NEA coverages, as seen experimentally. This indicates that, as already discussed for Model 1, it is necessary to introduce a second rule for the creation of forbidden sites for the adsorption of PO. After studying the behavior of the system for different alternatives, the following rule was developed:

Rule 2

If a site is surrounded by 2 adsorbed NEA up to 4th neighbors away, then it is forbidden for PO adsorption.

Some configurations illustrating this rule are shown in Fig. 11, and results from simulations using a model that included Rules 1 and 2 are presented in Fig. 12. We can see that the effect of adding this second Rule 2 is the appearance of the regression effect, with a proper behavior at low NEA coverages. Still, the PO yields are not sufficiently suppressed at high NEA coverages, and the enantioselectivity is not suppressed in that region.

At this point, a third rule was deemed necessary for the production of forbidden sites acting at high NEA coverages. Again, after many simulation attempts, the following rule was proposed:

Rule 3

If a site is surrounded by 5 or more 1st and 2nd neighbor NEAs, then it is forbidden for PO adsorption.

Some configurations illustrating this rule are shown in Fig. 13. The model that includes all three rules, Rules 1–3, constitute what we call Model 2. Some results from simulations using Model 2 are given in Fig. 14 for the TPD spectra, and in Fig. 15 for the integrated yields and enantioselectivities. The agreement between the predictions using Model 2 and the experimental data presented in Figs. 1 and 2 is quite good.

We can now discuss the effects of relaxing some of the complexities of Rule 1 for enantioselective sites by substituting it with the following:

Rule 1a

If a PO is adsorbed on a site B surrounded by 3 or more 2nd neighbor NEAs, all empty 2nd and 3rd neighbor sites become enantioselective for (S)-PO adsorption. In addition, the PO adsorbed on that site becomes strongly bounded to the surface.

The effects of this modification to Rule 1 are shown in Fig. 16. We see that the enantioselectivity corresponding to the low-temperature peak becomes too depressed, indicating that the creation of more enantioselective sites is needed. These extra enantioselective sites are included in Rule 1 as two 1st neighbor sites.

An alternative modification could be given as:

Rule 1b

If a PO is adsorbed on a site B surrounded by 3 or more 2nd neighbor NEAs, all empty 1st and 2nd neighbor sites and 2 of the 3rd neighbor sites become enantioselective for (S)-PO adsorption. In addition, the PO adsorbed on that site becomes strongly bounded to the surface.

The effects of this modification to Rule 1 are shown in Fig. 17. In this case, the enantioselectivities of the low- and high-temperature peaks become equal, which contradicts experiments. There is a strong basis to believe that all aspects of Rule 1 are necessary to take into account the synergetic production of enantioselective sites.

In all these simulations, no consideration has been given to the potential mobility of the NEA molecules on the surface. As a final test, some NEA re-arrangements were included under specific con-

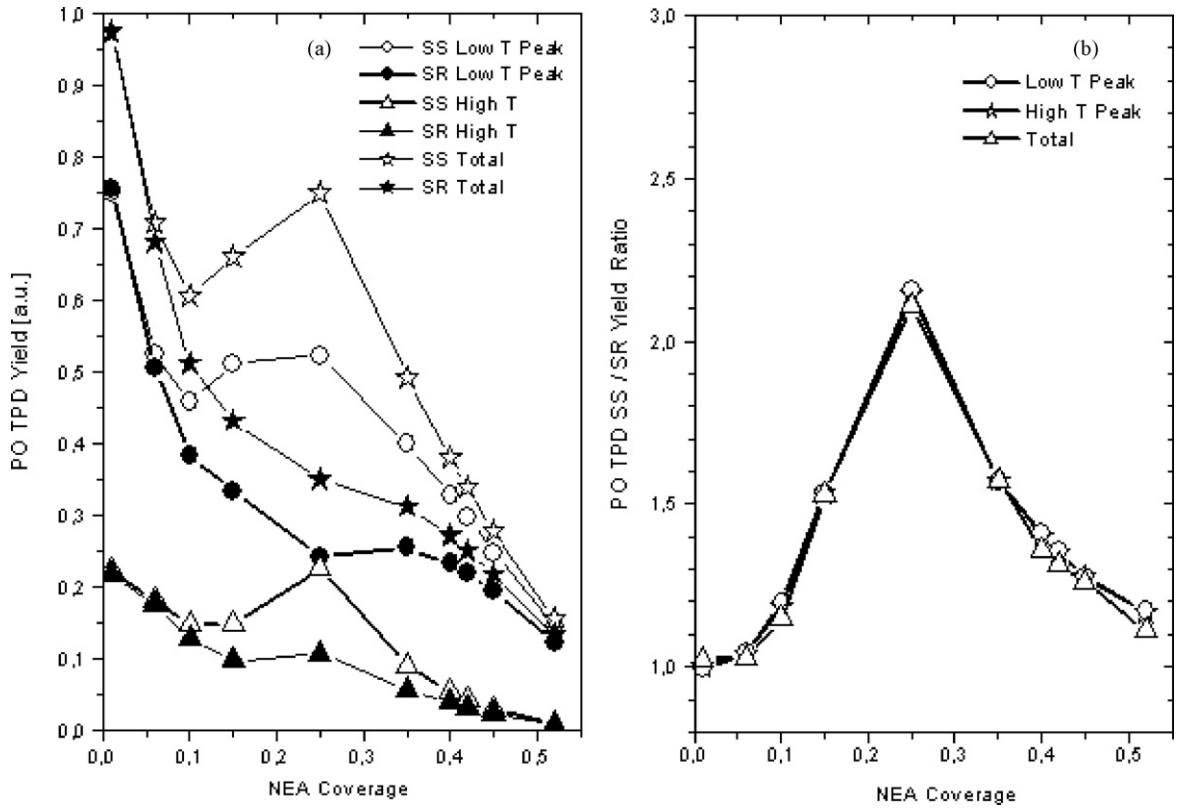

Fig. 17. Effect of relaxing Rule 1 to Rule 1b on the integrated spectra (a) and selectivity curves (b).

ditions in order to test if a synergetic configurational effect on both NEA and PO adsorbed molecules could simplify the complexity of the creation of forbidden sites given in Rules 2 and 3. To this end, Model 2 was modified in such a way as to allow NEA molecules to locally re-arrange in a more compact configuration as a region on the surface becomes too crowded, allowing them to also occupy B sites (a provision that blocks some sites for PO adsorption). The reproduction of the experimental data was not improved noticeably by this approach. Moreover, as soon as any condition for the creation of forbidden sites was relaxed, the agreement of the model predictions with the experimental data was lost in this case too.

4. Conclusions

The experimentally observed enantioselective behavior of the PO/(S)-NEA/Pt(1 1 1) system display some complex features that are quite revealing, and that cannot be simply explained by pairwise interactions between adsorbed species. It is necessary to consider cooperative effects in any model of these systems, where special configurations of adsorbed species modify the surface properties in such a way as to impart enantioselectivity toward one of the enantiomers of the probe (PO) molecule.

Two such cooperative models have been developed in the present work, identified as Models 1 and 2. Model 1 is among the simplest cooperative models that could be conceived. It provided a first crude approximation to the observed behavior, and was also useful to visualize what modifications were necessary to improve the predictive power of our modeling, among these the addition of weak and strong sites for PO adsorption, a mechanism to create forbidden sites for the adsorption of PO, and a mechanism for the creation of enantioselective sites for the selective adsorption of (S)-PO. This led to the advancement of Model 2, where the enantioselective properties of the surface change in a synergetic fashion upon interactions of PO and NEA molecules as their surface coverages increase. Model 2 reproduces satisfactorily all main observed trends in the experimental data.

In a comparison of Models 1 and 2, it can be said that the former has the advantages of being based on very simple rules and of providing a qualitative description of some of the features of the PO/NEA/Pt system observed experimentally. On the other hand, it has the disadvantage of providing only a very crude reproduction of the experimental data. Model 2, on the other hand, has the advantage of providing a very good quantitative prediction of the observed behavior, but the disadvantage of being based on complex rules not easy to rationalize in terms of understandable and intuitive surface chemistry. These rules should not be considered as a representation of what really happens on the surface, but as a clue to what is needed to reproduce the right behavior of the system.

Both these models represent a very first step toward the understanding of the process at a molecular level. They may help develop a better model where the advantages of Model 1 and Model 2 may be combined.

Acknowledgements

Financial support for the present work from CONICET (Argentina) and the US Department of Energy (USA) are gratefully acknowledged.

References

[1] T. Mallat, E. Orglmeister, A. Baiker, Chem. Rev. 107 (2007) 4863.
[2] F. Zaera, J. Phys. Chem. C 112 (2008) 16196.
[3] F. Zaera, Acc. Chem. Res. 42 (2009) 1152.
[4] J. Lai, Z. Ma, L. Mink, L.J. Mueller, F. Zaera, J. Phys. Chem. B 113 (2009) 11696.
[5] V. Humblot, S.M. Barlow, R. Raval, Prog. Surf. Sci. 76 (2004) 1.

[6] K.H. Ernst, Top. Curr. Chem. 265 (2006) 209.
[7] D. Stacchiola, L. Burkholder, W.T. Tysoe, J. Am. Chem. Soc. 124 (2002) 8984.
[8] F. Romá, D. Stacchiola, G. Zgrablich, W.T. Tysoe, J. Chem. Phys. 118 (2003) 6030.
[9] F. Romá, D. Stacchiola, G. Zgrablich, W.T. Tysoe, Physica A 338 (2004) 493.
[10] I. Lee, F. Zaera, J. Phys. Chem. B 109 (2005) 12920.
[11] I. Lee, F. Zaera, J. Am. Chem. Soc. 128 (2006) 8890.
[12] I. Lee, Z. Ma, S. Kaneko, F. Zaera, JACS 130 (2008) 14597.
[13] P. Szabelski, 227, Appl. Surf. Sci. 94 (2004).
[14] P. Szabelski, D.S. Sholl, J. Phys. Chem. C 111 (2007) 11936.
[15] P. Szabelski, D.S. Sholl, J. Chem. Phys. 126 (2007) 144709.
[16] J.L. Sales, R.O. Uñac, M.V. Gargiulo, V. Bustos, G. Zgrablich, Langmuir 12 (1996) 95.